Available online at www.sciencedirect.com
SCIENCE DIRECT®
Journal of Catalysis 236 (2005) 233–244
JOURNAL OF CATALYSIS
www.elsevier.com/locate/jcat

Tuning the structure, distribution and reactivity of polymerization centres of Cr(II)/SiO_2 Phillips catalyst by controlled annealing

Elena Groppo *, Carlo Lamberti, Giuseppe Spoto, Silvia Bordiga, Giuliana Magnacca, Adriano Zecchina *

Department of Inorganic, Physical and Materials Chemistry, and NIS Center of Excellence, University of Torino, via P. Giuria 7, I-10125 Torino, Italy

Received 30 June 2005; revised 30 August 2005; accepted 3 September 2005

Available online 4 November 2005

Abstract

The catalytic activity of two Cr(II)/SiO_2 samples obtained after two different controlled annealing procedures are discussed and compared. The combined application of FTIR spectroscopy and microgravimetric determinations demonstrated that the two Cr(II)/SiO_2 samples are characterized by a different relative population of the families of Cr(II) sites present on the silica surface and by a different catalytic activity toward ethylene polymerization. The different polymerization activity of the two catalysts is explained by supposing the presence of a distribution of Cr sites, all active but characterized by different turnover frequencies in ethylene insertion, which is related to the ability of Cr sites to insert up to three ligands into their coordination spheres. It is thus clear that the activation procedure plays an important role in determining the catalytic activity and the local structure of the active sites in the Phillips catalyst, which are strictly related. In this sense, the obtained results are of general validity, because identification of the structure–activity relation is a challenge common to many catalytic systems.

Keywords: Phillips catalyst; Ethylene polymerization; Turnover frequency; In situ IR; Activity

1. Introduction

The relation between the structure of the active sites and the catalytic activity is the core of the study in catalysis, and thus rational manipulation of the catalyst structure to improve catalytic activity is the main focus of catalyst design. However, achieving this goal is often troublesome, because the structure of the active sites on solid catalysts is often highly heterogeneous. The Cr/SiO_2 Phillips catalyst for ethylene polymerization (responsible for producing more than one-third of all the polyethylene worldwide [1–3]) represents a paradigmatic example, because, despite its apparent simplicity, a complete knowledge of the structure of the active sites is still missing. The difficulties encountered in investigating this catalyst derive mainly from the complexity of the chemistry of Cr grafted on the heterogeneous surface of the amorphous silica support. For this reason, over the years, the modification of catalytic activity of the system and the subsequent properties of the produced polymers have been obtained by modifying the silica support with promoters or by adopting different activation procedures mainly on the basis of phenomenological observations [1]. But these empirical approaches not based on a clear and comprehensive picture of the relation between the structure of the active sites, the polymerization activity, and the properties of the resulting polymers have unavoidable limitations. It must be stressed that this attitude is not confined to the Phillips catalyst and is widespread throughout the catalyst manufacturing industry.

To expand the previous statements, it is useful to recall that the Phillips-type catalysts have been historically obtained by grafting H_2CrO_4 on amorphous silica. A typical catalyst loading is between 0.2 and 1.0 wt% Cr, corresponding to 0.08–0.4 Cr atoms/nm^2, depending on the chosen reactor type. Following a calcination phase at high temperature, Cr is grafted in a hexavalent state, with a chromate structure. When brought into contact with ethylene at about 423 K, polymerization starts after a short induction period, needed to reduce Cr(VI) into

* Corresponding authors. Fax: +39 011 6707855.
E-mail addresses: elena.groppo@unito.it (E. Groppo), adriano.zecchina@unito.it (A. Zecchina).

0021-9517/$ – see front matter
doi:10.1016/j.jcat.2005.09.013

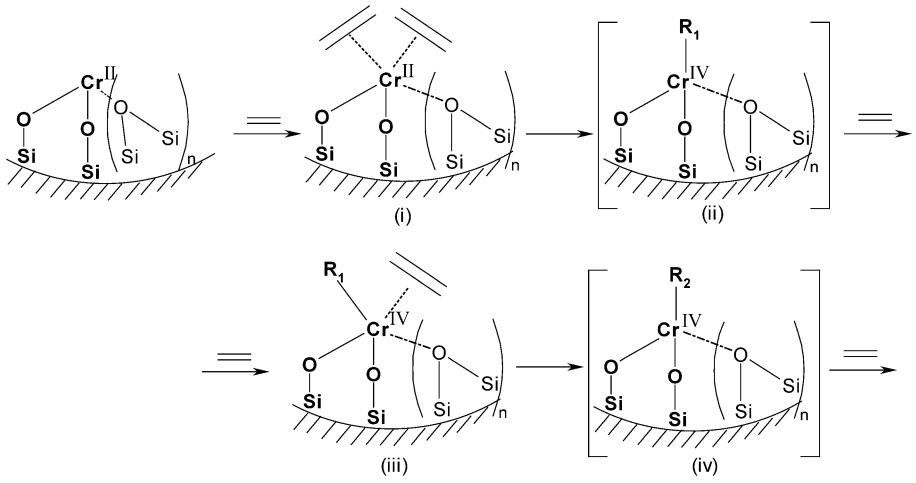

Scheme 1.

Cr(II) species [4]. In recent decades, low-valent Cr compounds, mainly Cr(III)–acetate [5–10], have been used as a starting material instead of Cr(VI) compounds, due to environmental and safety considerations, being that the water-soluble and mobile Cr(VI) species are extremely toxic. In these cases, it has been demonstrated that Cr(III)–acetate is converted first into bulky CrO_3 through oxidative decomposition and then into chromate species [5–10], thus basically returning to the starting point of the Cr(VI)-derived versions of the Phillips catalyst.

The Cr(II) species are only the precursors of the real catalytic sites, which in fact derive from them on subsequent interaction with ethylene. The structure of the real active sites (whose formation, unlike that of other polymerization catalysts, does not require the intervention of activators) is the most controversial topic of this catalyst. The induction period is absent when polymerization is done by prereducing the oxidized version of the catalyst in CO at 623 K. This system represents a model version of the industrial catalyst and is more suitable for spectroscopic investigations [1,4,11–15]. Without entering into a detailed discussion of the polymerization mechanism (for which the reader is referred to more specialized literature recently reviewed in Ref. [1]), the initiation stage of the polymerization reaction on the reduced Phillips catalyst can be generally represented as in Scheme 1. The precursor of the active site is a Cr(II) species, whose coordination sphere is composed of two strong oxygen ligands and a variable number n of weaker ligands, such as the siloxane groups present on the amorphous silica surface (with n varying in the range 0–4). The first step (i) is the C_2H_4 adsorption on the Cr(II) sites [16], followed by the formation of the first product R_1, step (ii) in Scheme 1. Uncertainty exists about the nature of R_1, and many structures have been proposed in the literature [1,17–23], all having in common the fact that the valence state of Cr is (IV), and hence the formation of CrR_1 species is an oxidative addition of two ethylene molecules. The reaction then proceeds via the coordination of a new C_2H_4 molecule, step (iii) in Scheme 1, and its insertion into R_1, which grows out of one monomeric unit [step (iv) in Scheme 1]. It is quite conceivable that during these steps the Cr-siloxane distances can variably relax because of the coordination/reaction involving the Cr centre.

Whereas the oxidation state of the Cr precursors in the model $Cr(II)/SiO_2$ system is now well established (mainly divalent), conversely their structure (i.e., number, type, and position of weaker ligands; see Scheme 1) remains unclear. Several spectroscopic techniques have been adopted to clarify the distribution of coordination environment of Cr(II), including UV–vis DRS [1,12,13,24,25], FTIR spectroscopy of adsorbed probe molecules (CO, NO, CO_2, N_2O, pyridine, and, more recently, H_2 and N_2) [1,16,17,26–38], Raman spectroscopy [1,25,39–42], XAS [1,24,43], and XPS [1,15,44]. The scenario emerging from all of these results is extremely complex, reflecting the high heterogeneity of the silica support [1]. Different families of Cr(II) sites have been classified, according to their coordination sphere. Following the nomenclature adopted previously [1,9,17,27,30,36–38,45], we can basically distinguish three families of Cr(II) ions: Cr^{II}_A sites (able to coordinate up to two CO molecules at room temperature [RT]), Cr^{II}_B sites (able to coordinate only one CO molecule at RT), and Cr^{II}_C sites (adsorbing CO only at 77 K). These species are characterized by differing polarizing ability ($Cr^{II}_C > Cr^{II}_B > Cr^{II}_A$) and differing propensity to give d–π back-donation ($Cr^{II}_C \ll Cr^{II}_B < Cr^{II}_A$).

It has been hypothesized that thermal annealing in vacuum at high temperatures modifies the relative population of the Cr(II) families [1,17,27,36,46], because it favors the progressive sinking of the Cr sites into the flexible surface of the amorphous silica, with the less coordinatively saturated ones (Cr^{II}_A) the most affected. It was also reported that the catalyst obtained after prolonged annealing at high temperature was less active than the standard one (and hence the treated sample was called “deactivated”) [17,27,36,46], and this led to the conclusion that the only sites active in the ethylene polymerization are the Cr^{II}_A sites. Although the conclusion concerning the null activity of Cr^{II}_C sites is certainly correct, the same hypothesis concerning Cr^{II}_B sites was not fully proved.

At this point it is useful to emphasize that a direct relation between the structure of the Cr sites and the catalytic activity has never been subjected to a detailed investigation. The absence of studies on this topic have precluded the design of catalysts with performance not based simply on empirical phenomeno-

logical observations or on trial-and-error approaches. In this work we investigate more systematically the effect of varying a fundamental parameter of the Phillips catalyst preparation—the annealing temperature of the prereduced sample—on the structure and the activity of Cr sites. We demonstrate that Cr^{II}_A and Cr^{II}_B sites are both active in the ethylene polymerization, but with distinctly different turnover frequencies (TOFs) for the monomer insertion. We conclude that, due to the different activity, a change in the relative population of the Cr sites through different activation procedures affords a means of controlling the properties of the resulting polymers. In particular, the catalytic activity (as determined during the first minutes of the polymerization reaction) of different $Cr(II)/SiO_2$ systems subjected to different activation procedures can vary greatly. This time scale, although far from that adopted in industrial applications, is the only one that allows us to advance a hypothesis on the roles of the different Cr sites in polymerization. In fact, we demonstrate that during the first 2 min of reaction at RT, the catalytic behavior of catalysts subjected to different activation procedures is exactly the opposite of those measured at greater times (and forming the basis of the commonly accepted model present in the literature) [17,27,36,46].

Another conclusion emerging from this work is that an accurate control of the annealing procedures allows us to elucidate the relation between the structure of the active sites and the catalytic activity. On this basis, it is also possible to design in a rational way new versions of the Phillips catalyst responsible for the production of polyethylenes characterized by desired properties. These results are of general validity and can be extended to several other catalytic systems as well.

2. Experimental

2.1. Sample preparation

The $Cr(II)/SiO_2$ samples used for the CO adsorption and C_2H_4 polymerization experiments followed by IR spectroscopy and for the microgravimetric measurements were prepared by impregnating a silica-aerosil (surface area of about 380 m^2/g) with H_2CrO_4 up to a 1 wt% Cr loading. The impregnated silica was then dried at RT and pressed into a pellet. For the IR study of N_2 adsorption, silica-aerogel [47] (characterized by a higher surface area, about 700 m^2/g, and lower scattering properties) was used as support to allow better detection of the weak bands of the $Cr(II)\cdots N_2$ complexes [1,16,41,42]. The silica-aerogel monolites were impregnated with a solution of CrO_3 in CH_3CN (resulting in a 1 wt% Cr loading), then dried at RT, reduced in powder, and pressed into a thick pellet (∼0.5 mm), as discussed elsewhere [1,16,41].

2.2. IR experiments

To perform the IR experiments, the catalyst pellets were transferred into an IR cell designed to allow thermal treatments in the 1000–77 K range, either under vacuum or in presence of a desired equilibrium pressure of gases. The samples were activated following two different procedures. The first (standard) procedure involved activation at 923 K, calcination in O_2 at the same temperature for 1 h, reduction in CO at 623 K for 1 h followed by CO removal at the same temperature, and cooling to RT. The second (high-temperature) procedure differed from the standard procedure in that in the last step the sample was heated in vacuum at 923 K for 1 h before cooling to RT. During this step the valence state of Cr does not change. In the following the samples obtained according to the first or second procedure are denoted as "standard" catalyst (**S**) or "thermally treated" (annealed) catalyst (**T**), respectively. It is worth underlining that the high-temperature treatment (annealing) adopted here is less drastic than that described elsewhere [17,27,36,46], which led to fully deactivated samples.

CO and N_2 adsorption and C_2H_4 polymerization experiments were performed on three different pellets; however, each experiment was performed on the same sample treated following the two activation procedures in sequence. This means that the comparison of the intensity of the ν(CO), $\nu(N_2)$ and $\nu(CH_2)$ stretching bands directly gives the relative amount of adsorbed CO and N_2 and of polyethylene formed on the two catalysts. The FTIR spectra were collected on a Bruker IFS-66 spectrophotometer equipped with a MCT cryodetector, at 1 cm^{-1} resolution.

2.3. Microgravimetric experiments

For the microgravimetric experiments, the pellets were transferred into the microbalance inside a quartz reactor allowing thermal treatments up to 1300 K either in vacuum or in controlled atmosphere. The samples were activated following the same procedures discussed in Section 2.2. The microgravimetric measurements were performed on an IGA002 microbalance by Hiden.

3. Results and discussion

3.1. How the activation procedure influences the structure of the Cr(II) precursor sites: an FTIR investigation

FTIR spectroscopy of probe molecules has been largely used in the past to highlight the coordination environment of the Cr(II) sites in the Phillips catalyst [1,17,26–38]. In this section we compare the results of CO and N_2 adsorption, at RT and at 77 K, on samples obtained following the two different activation procedures discussed in Section 2.2. CO and N_2 were chosen among all of the probe molecules adopted in the past because their adducts with the Cr^{II}_A and Cr^{II}_B families of sites have distinctly different vibrational signatures [16]. The results on CO adsorption have been discussed previously [1], but are presented here in a concise way to elucidate the evolution of the Cr structure as a function of annealing and to allow interpretation of the results obtained with N_2 adsorption. The complete assignment of all of the spectroscopic features can be found elsewhere [1].

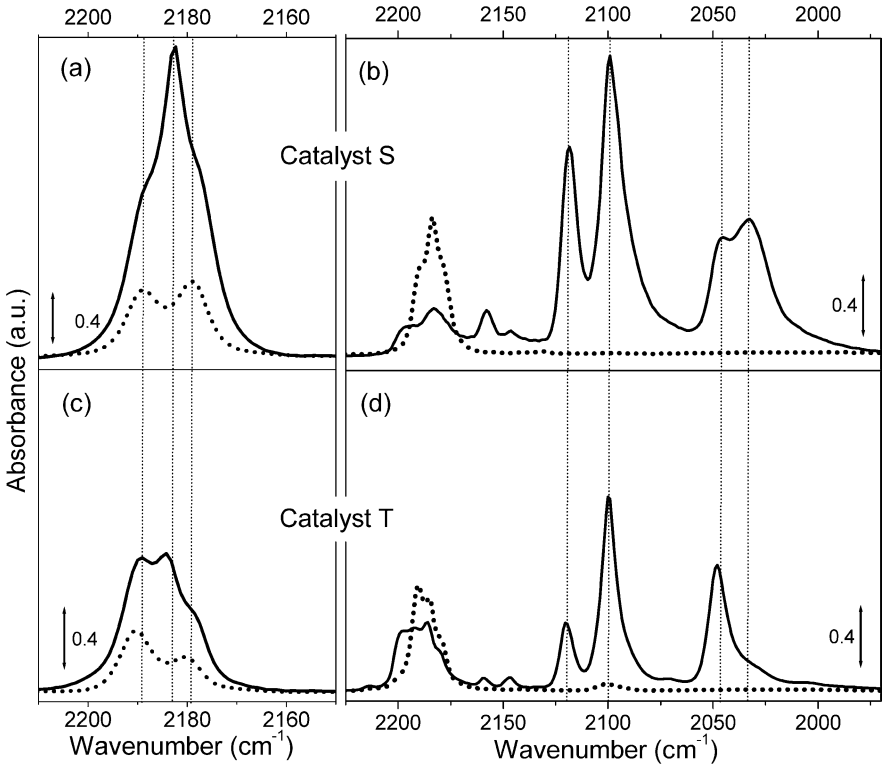

Fig. 1. (a) Background subtracted FTIR spectra, in the C–O stretching region, of CO adsorbed at RT on catalyst **S**. Full and dotted curves correspond to equilibrium pressure $P_{CO} = 40$ Torr and $P_{CO} = 10^{-3}$ mbar, respectively. (b) As part (a) for CO adsorbed at 77 K on catalyst **S**. (c) The same of (a) but for catalyst **T**. (d) The same of (b) but for catalyst **T**. For clarity, only the spectra corresponding to the highest and the lowest CO coverages are reported. Dotted vertical lines, centered on the main spectroscopic features of catalyst **S**, show the frequency shifts which characterize the same bands in the case of catalyst **T**.

3.1.1. Probing Cr(II) sites by CO adsorption at RT and 77 K: formation of Cr(II)···(CO)$_n$ adducts

As it is well known, the interaction of CO with a standard Cr(II)/SiO_2 sample (equilibrium pressure, $P_{CO} \sim 40$ Torr) at RT results in the so-called "RT triplet," composed of a component at 2191 cm^{-1} and a doublet at 2184–2178 cm^{-1} (represented by the solid-line spectrum in Fig. 1a). Note that all of these bands are at $\tilde{\nu}$(CO) higher than that of CO gas [1,9,17,27,30,36,37,45], as expected for carbonylic complexes dominated mainly by polarization forces [48]. According to the literature, the triplet is attributed to a mixture of $Cr^{II}_B\cdots$CO (band at 2191 cm^{-1}) and of $Cr^{II}_A\cdots(CO)_2$ complexes (doublet at 2184–2178 cm^{-1}). At low P_{CO} (the dotted-line spectrum in Fig. 1a), only two bands are present: one, still at 2191 cm^{-1}, belonging to residual $Cr^{II}_B\cdots$CO adducts and a second new component at 2180 cm^{-1}, assigned to $Cr^{II}_A\cdots$CO complexes deriving from $Cr^{II}_A\cdots(CO)_2$ by the loss of one CO molecule. According to this interpretation, it is evident that Cr^{II}_A sites are more coordinatively unsaturated than Cr^{II}_B sites, because they are able to adsorb up to two CO molecules at RT and present a higher tendency to give d–π interactions, as they are characterized by lower $\tilde{\nu}$(CO).

The RT triplet is partially eroded by decreasing the temperature to 77 K, with formation of a complex series of bands in the 2140–2050 cm^{-1} range, that is, at $\tilde{\nu}$(CO) lower than that of the CO gas, as shown in Fig. 1b, where the dotted and full lines represent the spectra obtained at low and high P_{CO}, respectively. An additional band, absent at RT, is observed at about 2200 cm^{-1}. These spectra, which are well known and perfectly reproducible, have been the subject of much controversy in the past [17,26,27,30,36,38,49,50]. A detailed assignment of all of the bands, as has been done previously [1], is not the aim of this work. Here we just recall that the complex spectrum in the 2140–2050 cm^{-1} interval can be explained in terms of the superimposition of the modes of a mixture of $Cr^{II}_A\cdots(CO)_3$ and $Cr^{II}_B\cdots(CO)_3$ species (both with symmetry lower than that of C_{3v}), formed by the insertion of additional CO ligands into a preexisting carbonyl adduct through displacement of weaker ligands (siloxane bridges present on the silica surface; see Scheme 1). Cr^{II}_B sites rapidly add two more CO molecules with increasing CO pressure (or decreasing temperature), whereas the addition of a third CO molecule on Cr^{II}_A sites is more difficult [1]. The band at about 2200 cm^{-1} has been attributed to the $\tilde{\nu}$(CO) of CO ligands probing a third family of coordinatively less unsaturated sites, substantially inactive at RT but with enhanced polarizing ability (Cr^{II}_C sites) [1,36,38].

Repeating the same set of IR experiments on sample **T** produced a dramatic reduction of the CO RT triplet (Fig. 1c). Note that the effect of the thermal treatment on A and B sites is not the same, in that the Cr^{II}_A family is preferentially affected. Moreover, closer inspection of the spectra reported in Figs. 1a and 1c shows that passing from catalyst **S** to catalyst **T** affects not only the relative intensity of the bands, but also their frequency. Although small (about 2 cm^{-1}), a shift of the carbonyl bands can be appreciated by referring to the dotted vertical lines in Fig. 1. In particular, all of the components of the CO triplet

for **T** sample are shifted to higher-frequency values. An analogous behavior is shown by the spectra of CO adsorbed at 77 K (Figs. 1d and 1b). As widely discussed [1], on the **T** sample the concentration of $Cr^{II}_A\cdots(CO)_3$ species (2120, 2100 and 2035 cm^{-1} components) is greatly decreased with respect to the **S** sample, and the remaining low-frequency triplet (2120, 2100, and 2048 cm^{-1}) substantially belongs to $Cr^{II}_B\cdots(CO)_3$ species.

The conclusion emerging from these results is that both the **S** and **T** catalysts contain three families of sites, whose proportion can be changed by annealing. In more detail, the thermal treatments in vacuum of Cr(II)/SiO_2 system favors a complex rearrangement (relaxation) of the surface, which has two main consequences. First, most of the more coordinatively unsaturated Cr^{II}_A sites sink into the silica surface, increasing crystal field stabilization. Because the valence of Cr remains unchanged, this means that, due to surface rearrangement, weak SiOSi ligands enter the coordination sphere of chromium. This is confirmed by the change in color of sample **T**, which assumes a darker-blue shade with respect to catalyst **S**, indicating an increase in the coordination sphere of the Cr(II) ions [1]. The large increase of the Cr^{II}_C family and the smaller increment of the Cr^{II}_B center population is simply the result of a multiple evolution in terms of $nCr^{II}_A \rightarrow nCr^{II}_B$ and $mCr^{II}_B \rightarrow mCr^{II}_C$ transformation, with $m \sim n$. This complex evolution involves relaxation of the external layers of the silica support. This also influences the sites not transformed by the annealing process, thus explaining the small shifts in the frequency values characterizing all of the CO bands at both RT and 77 K.

3.1.2. Probing the Cr(II) sites by N_2 adsorption at RT and 77 K: formation of Cr(II)$\cdots(N_2)_n$ adducts

The effect of the thermal treatment in vacuum on the local structure of the Cr(II) sites is confirmed by the results of the IR spectra of adsorbed N_2 (see Fig. 2). In relation to this, it is noteworthy that we recently reported the first Raman and IR evidence of Cr(II)$\cdots(N_2)_n$ complexes formed at RT on a "standard" Cr(II)/SiO_2 system [16,41,42]. In this respect, it is worth recalling that only a few examples of N_2 complexes formed on oxide surfaces [51,52] or on metal-exchanged zeolites [48, 53–60] have been reported to date, and that most of these are formed in low-temperature and/or high-pressure conditions. It was demonstrated that at RT, only one N_2 molecule is adsorbed on both Cr^{II}_A and Cr^{II}_B families, giving rise to two $\tilde{\nu}$(NN) peaks at 2328 ($Cr^{II}_A\cdots N_2$) and 2337 cm^{-1} ($Cr^{II}_B\cdots N_2$), respectively (indicated by the dotted line in Fig. 2a). The very small $\Delta\tilde{\nu}$(NN) observed for the Cr(II)$\cdots N_2$ adducts (-3 and $+6$ cm^{-1}, respectively) with respect to the gas phase apparently conflicts with the stability of these species. It has been suggested that this small shift is the result of a balance between the positive shift induced by polarization forces and the opposite effect due to σ–π overlap forces. At lower temperature (higher P_{N_2}), a second N_2 molecule was inserted into the $Cr^{II}_A\cdots N_2$ complex, giving rise to a band at 2331 cm^{-1} (the solid line in Fig. 2a), whereas Cr^{II}_B sites remain able to coordinate only one N_2 molecule (band shift from 2337 to 2340 cm^{-1}; the solid line in Fig. 2a).

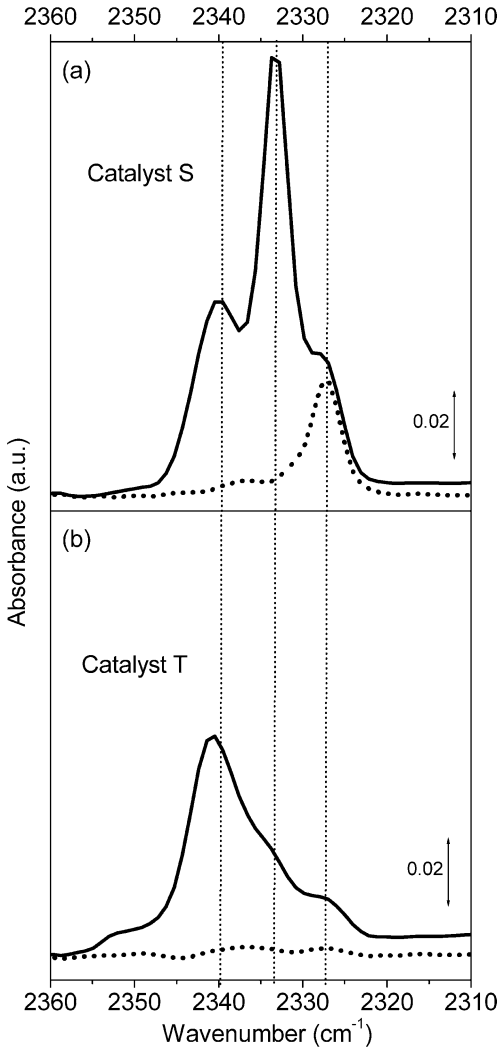

Fig. 2. (a) Background subtracted FTIR spectra, in the N≡N stretching region, of N_2 adsorbed on catalyst **S** ($P_{N_2} = 40$ Torr). Full curve, adsorption at 77 K; dotted curve, adsorption at RT. (b) The same of (a) but for catalyst **T**. Dotted vertical lines, centered on the main spectroscopic features of catalyst **S**, show the frequency shifts which characterize the same bands in the case of catalyst **T**.

Fig. 2b reports the same experiment performed on sample **T**. At RT (the dotted curve in Fig. 2b), the intensity of the peaks attributed to $Cr^{II}_A\cdots N_2$ and to $Cr^{II}_B\cdots N_2$ adducts is negligible. This confirms that the thermal treatment converts most of the Cr^{II}_A sites into more shielded sites, unable to coordinate N_2 molecules at RT. When the temperature is decreased down to 77 K, an intense band grows up at about 2340 cm^{-1}, becoming the dominant feature of the spectrum. This peak, which is a little more intense than that observed on sample **S** and assigned to $Cr^{II}_B\cdots N_2$ complexes, presents a distinct shoulder at 2353 cm^{-1}. In analogy with the CO case, this shoulder is tentatively assigned to $Cr^{II}_C\cdots N_2$ complexes. At the same time, a weak band arises at about 2334 cm^{-1}, which may be the weak manifestation of the residual $Cr^{II}_A\cdots(N_2)_2$ adducts, shifted upward of 3 cm^{-1} with respect to the standard case (see the dotted vertical lines in Fig. 2). Finally, as previously reported for the case of the standard Cr(II)/SiO_2 sample [16], at the highest N_2 pres-

sures a new broader absorption develops at ca. 2325 cm^{-1}, that is the spectroscopic manifestation of the physisorbed N_2.

The conclusions derived from the analysis of the FTIR spectra of adsorbed N_2 well agree with those obtained in the case of CO adsorption. In particular, it is confirmed that on high-temperature annealing, the concentration of the Cr^{II}_A species decreases dramatically, whereas that of Cr^{II}_C families increases and a slight increase of Cr^{II}_B seems to occur. In other words, the hypothesis that high-temperature annealing of reduced samples induces a complex $Cr^{II}_A \rightarrow Cr^{II}_B \rightarrow Cr^{II}_C$ transformation is thus confirmed. It is notable that oxidation of the annealed samples followed by reduction with CO at 350 °C gives a Cr(II)/SiO_2 system whose spectroscopic features on N_2 adsorption are indistinguishable from those of the standard sample. This means that the effect of the annealing is fully reversible. It is also useful to underline that the local structure of the main Cr families changes slightly on heating, justifying the little but well-reproducible frequency shifts of the adduct vibrational features.

3.2. How controlled annealing of the reduced precursors influences the polymerization activity of Cr(II)/SiO_2

From the spectroscopic results discussed so far, it is clear that the relative population of Cr^{II}_A, Cr^{II}_B, and Cr^{II}_C sites can be tuned by controlled annealing. The question now is whether we can use this approach to tune the catalytic activity toward ethylene polymerization. If we can, then we have sufficient knowledge to modify, in a rational way, the properties of the catalyst. To prove the veracity of this statement, our next goal is to evaluate the effect of controlled annealing on the catalytic activity of the two samples. This experiment not only can validate the foregoing hypothesis, but also can provide information on the specific activity of the different Cr sites. Toward this purpose, we measured the weight variation of samples **S** and **T** as a function of time during the ethylene polymerization reaction at RT, using a microbalance operating under controlled atmosphere (see Section 3.2.1). The polymerization reaction was conducted at a constant C_2H_4 pressure of 100 Torr (see Fig. 3a). The microgravimetric results obtained during the first minutes of the reaction were then compared with the FTIR spectra of the growing polymeric chains formed under identical conditions, with the aim of finding a correlation between the catalytic activity and the spectroscopic features of the resulting polymers (see Section 3.2.2).

3.2.1. Microgravimetric results

Fig. 3b compares the microgravimetric results obtained on the two catalysts activated with the two different procedures. The variation of the sample weight is reported as a function of the polymerization time. The zero-time corresponds to the C_2H_4 admission in the reactor; see Fig. 3a for the corresponding equilibrium pressure. Fig. 3c shows the first derivative of the curves reported in Fig. 3b. Starting with the discussion of catalyst **S** (full line), three main regions can be identified: (1) a "jump" region (0–30 s), in which we observe a sudden increase in the sample weight; (2) a region in which the sample weight increases in a progressive manner (30–650 s); and (3) a region

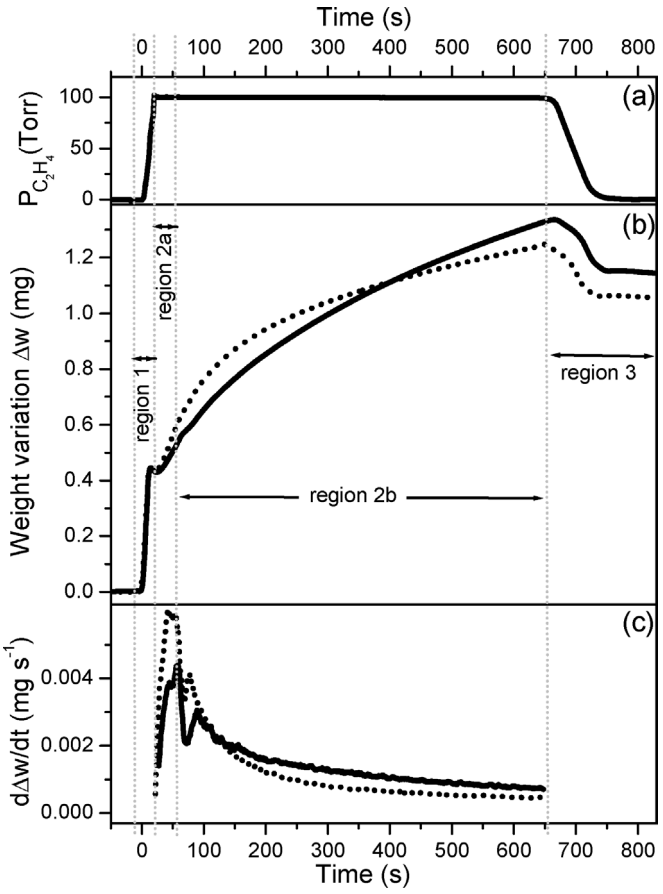

Fig. 3. (a) C_2H_4 pressure variation inside the reactor adopted for the microgravimetric experiment during the polymerization reaction at RT. (b) Weight uptake of the Cr(II)/SiO_2 samples during the ethylene polymerization as a function of time. Regions 1 and 2 refer to the initiation and propagation phases of the polymerization reaction, respectively, whereas region 3 corresponds to the stop of the reaction, obtained by evacuating the reactor (see explanation in the text). (c) First derivative of the curves reported in the part (b) (for simplicity only data referring to region 2 are shown). Full line, sample **S**; dotted line, sample **T**.

corresponding to the stop of the reaction, obtained by a sudden decrease of the C_2H_4 pressure from 100 Torr to 0 (650 s–end) (see Fig. 3a).

Starting with the region 1, the sharp jump observed in the sample weight on ethylene admission into the reactor is due mainly to the superimposition of two phenomena: (a) coordination of ethylene on Cr(II) sites [species (i) in Scheme 1] and (b) formation of the first polymeric products on few Cr(II) sites [species (ii) in Scheme 1], those faster in the C_2H_4 insertion. Assuming that region 1 reflects mainly the formation of species (i) in Scheme 1, from the weight "jump" ($\Delta w = 0.450$ mg) we can in principle obtain an estimation of the fraction of Cr sites able to adsorb ethylene, with the total number of Cr atoms present in the sample known (1.4×10^{19} atoms). By assuming that diethylene complexes [structure (i) in Scheme 1] are by far the most abundant species, as demonstrated previously [16], we obtain that a fraction not far from 35% of the total Cr sites are contributing to the weight jump. Because a minor fraction of Cr(II) species may adsorb only one C_2H_4 molecule, the frac-

tion of 35% of the total Cr sites represents a lower limit for the sites able to coordinate ethylene at RT.

After the first 30 s of contact, we observe a progressive and gradual increase in the sample weight, due to the gradual growth of the polymer chains on the active Cr(II) sites (region 2 in Fig. 3). The slope of the curve (i.e., its first derivative; see Fig. 3c) represents the number of ethylene molecules inserted per second on the whole number of active sites. This value is proportional to the TOF via the unknown fraction of active sites. It is clear that the TOF increases sharply in the first 50–60 s of the reaction (region 2a) and then rapidly decreases (beginning of region 2b), reaching an almost steady value for longer polymerization times (end of region 2b). In these conditions, we estimate a polymerization speed (at 300 K and 100 Torr of ethylene) of about 0.0015 C_2H_4 molecules per second per Cr sites. The behavior characterizing region 2a can be explained only by assuming that the number of active sites is increasing in the first stages. This implies that in this time interval, the really active sites are built via oxidative addition starting from the precursor Cr(II) species [steps (i) → (ii) in Scheme 1]. The rapid decrease of the TOF after the first 50–60 s (region 2b), may be due to a "poisoning effect" caused by the growing polymeric chains (through, e.g., limited accessibility of a fraction of the Cr sites for the C_2H_4 molecules), which should take a sort of percolative path. The weight uptake in this time interval corresponds to the growth of living polymeric chains [steps (iii) and (iv) in Scheme 1].

Finally, when the polymerization is stopped by evacuating the cell (region 3 in Fig. 3a), we observe a decrease in sample weight (Fig. 3b). This is due to the removal of the ethylene molecules π-bonded on the Cr(II) sites that have not been able to start the polymerization process. On the basis of the considerations developed earlier, the weight decrease on outgassing ($\Delta w = -0.187$ mg) represents, in absolute value, 41% of the positive weight jump characterizing region 1. In other words, 41% of the C_2H_4 molecules initially adsorbed have just formed weakly adsorbed complexes and have not started the polymerization reaction. This means that the remaining 59% of ethylene molecules have been converted into the precursor R_1 characterizing species (ii) in Scheme 1. This fraction can be directly converted into the fraction of Cr(II) sites able to pass from structure (i) into structure (ii) in Scheme 1, that is, the fraction of active sites. Incertitude occurs when we try to estimate the active sites as a fraction of the total number of Cr sites present in the sample and not as a fraction of the sites able to coordinate ethylene at RT. Assuming that diethylene complexes are formed on 35% of the total Cr sites, vide supra the discussion of the jump, the fraction of active sites is 21% of the total Cr atoms. Because a minor fraction of Cr(II) species may coordinate only one ethylene molecule, this value must be considered a lower limit. Using this value in the evaluation of the TOF, we obtain that, in steady-state conditions, the TOF is about 0.0075 C_2H_4 s^{-1} for polymerization conducted at 300 K and 100 Torr of ethylene. This value is lower than those reported in the literature (e.g., 0.44 C_2H_4 s^{-1} at 353 K and $P_{C_2H_4}$ of 500 Torr [61]; 0.26 C_2H_4 s^{-1} at 300 K and $P_{C_2H_4}$ of 1 atm [62]), but the comparison is not direct, because the literature values were obtained under different temperature and pressure conditions and on catalysts activated following different procedures. Finally, it is noteworthy that the value of active site determined here is in fair agreement with the estimation recently obtained by XANES spectroscopy [43]. In that work, by comparing the integrated area of the Cr(II) pre-edge fingerprint at 5996 eV in the catalyst before and after polymerization, we estimated that about 25% of the original Cr(II) sites were involved in the polymerization at RT.

Comparing the sample weight variation as a function of the polymerization time for catalysts **S** and **T** (the solid and dotted curves in Fig. 3b, respectively), we can state the following considerations:

(i) The weight "jump" (region 1 in Fig. 3b) is virtually equivalent in the two samples.
(ii) During the first 120 s the rate of weight increment is higher for sample **T** than for sample **S**.
(iii) After the first 120 s, the slope of the curve for sample **T** begins to decrease, and sample **S** becomes more active (the fact being more evident in Fig. 3c); the integrated weight variation becomes greater for sample **S** for times greater than 400 s (Fig. 3b).
(iv) The weight decrease on outgassing is equivalent for the two samples, a fact that, combined with consideration (i), suggests that the fraction of sites involved in the polymerization reaction is almost the same in the two cases.

The behavior observed for polymerization times >120 s agrees perfectly with results in the literature indicating that catalyst **T** is less active (deactivated) than catalyst **S** [17,27,46]. The behavior of the two catalysts during the first minutes of the polymerization reaction is, on the contrary, exactly the opposite of that proposed in the published literature and merits a special discussion.

We can explain the different polymerization rates of the two catalysts by supposing that the Cr^{II}_A and Cr^{II}_B families are characterized by different rates in the ethylene insertion and by different activation energies. From the spectroscopic results given in Section 3.1, it is clear that the two catalysts differ mainly in terms of the concentration of Cr^{II}_A sites (which are almost absent in sample **T**) and the local structure of the Cr^{II}_B sites. Comparing the two curves reported in Fig. 3b, we hypothesize that the Cr^{II}_B sites are the first to start the polymerization reaction and insert ethylene molecules very rapidly in the growing chains. The thermal annealing causes little increase in the fraction of Cr^{II}_B sites and changes their structure only slightly. This explains both the higher TOF of sample **T** in the first 120 s and the similar intensity of the weight jump in the two samples, notwithstanding the lower concentration of Cr sites able to adsorb C_2H_4 molecules in sample **T**. The decrease in the number of C_2H_4 adsorbed molecules, in fact, is replaced by an increase in the number of inserted C_2H_4 in the polymeric chains, so that the resulting weight variation is almost the same as that observed in the standard sample. However, after a certain point (i.e., after overcoming the activating energy barrier), the Cr^{II}_A sites also begin to slowly polymerize and the standard sample,

which has numerous Cr^{II}_{A} sites, becomes more active. For sample **T**, the almost complete lack of Cr^{II}_{A} sites may account for the lower final activity.

3.2.2. FTIR results

The first steps in the polymerization reaction on both catalysts have been evaluated by time-resolved FTIR spectroscopy, with the aim of studying the vibrational features of the first polymeric chains, as reported in Fig. 4. Because of the high intensity of the bulk modes of the silica support below 1500 cm^{-1}, only the frequency region corresponding to the CH_2 stretching modes of the growing polymeric chains is accessible. This region, even if of particular interest, is seldom used for diagnostic purposes in the literature, mainly because the strong intensity of the corresponding features generally results in saturation of the corresponding bands.

The sequences of spectra reported in Figs. 4a and 4b were collected every 20 s during the first steps of the ethylene polymerization on catalyst **S** and catalyst **T**, respectively. The last spectrum corresponds to a polymerization time of 2 min. The spectra are characterized by two bands, assigned to the antisymmetric (2926 cm^{-1}) and symmetric (2856 cm^{-1}) stretching vibrations of the CH_2 groups of the growing polymeric chains [1,17,38]. The weak absorption around 3000 cm^{-1} is due to the C_2H_4 π-bonded to the Cr(II) sites [16]. As discussed in the Experimental section, the experiments were performed on the same Cr/SiO_2 pellet subjected to the two different activation procedures, so that the comparison of the intensity of the $\nu(CH_2)$ stretching modes directly gives the relative amount of PE formed on the two catalysts. Comparing the two sequences of spectra obtained for catalysts **S** and **T**, it is evident that the two bands related to the $\tilde{\nu}(CH_2)$ stretching modes grow faster for catalyst **T** than for catalyst **S**. This behavior strongly supports the idea that sample **T** is more active during the initial stages of the polymerization reaction, as suggested by the microgravimetric results (region 2a in Fig. 3).

A closer inspection of the most intense spectra of the two sequences reported in Figs. 4a and 4b and compared in Fig. 5 (bottom part) reveals that the CH_2 stretching bands of the polymer chains growing on sample **T** are much more narrow and shifted to lower frequency than those growing on sample **S**. For comparison, Fig. 5 (top) also reports the IR spectra of tritriacontane (a long alkane characterized by a ratio $CH_3/CH_2 = 2/31$) and *n*-hexadecane (a shorter alkane characterized by a ratio $CH_3/CH_2 = 2/14$). Table 1 reports the peak positions of the $\nu(CH_2)$ stretching modes for the PE chains growing on catalysts **S** and **T** and compares them with those of reference samples (i.e., PE in the crystalline and liquid phase, *n*-hexadecane and tritriacontane). It is noteworthy that the vibrational features of CH_3 groups, $\tilde{\nu}_a(CH_3)$ and $\tilde{\nu}_s(CH_3)$ at 2955 and 2873 cm^{-1}, respectively, are already observable in the spectrum of tritriacontane, that is when the CH_3/CH_2 ratio is very low.

To explain the differences between the PE chains grown on **S** and **T** samples, it is useful to recall that previous IR studies [63–69] have shown that the CH_2 stretching frequencies (in both the symmetric and antisymmetric modes) are sensitive indicators of lateral interactions between long *n*-alkyl and PE chains and also provide a qualitative indication of the conformational disorder. In more detail, a shift toward higher wavenumbers indicates an

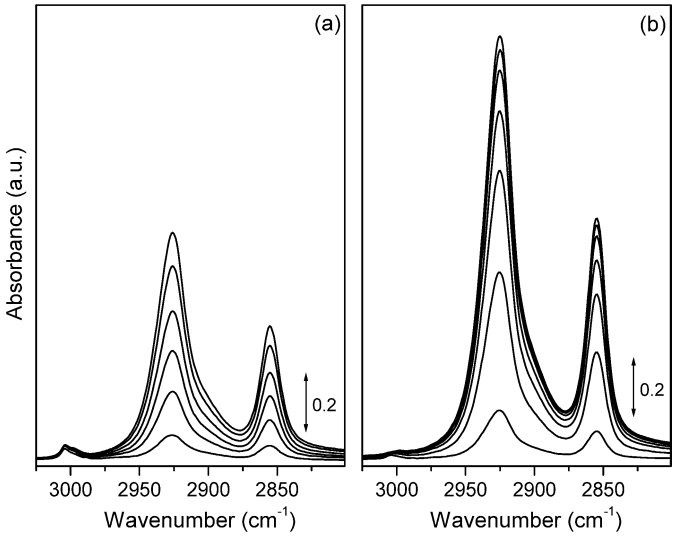

Fig. 4. (a) Time-resolved FTIR spectra, in the $\nu(CH_2)$ region, of the polymeric chains growing on sample **S**. Each spectrum has been collected every 20 s. (b) The same of (a) for catalyst **T**. As the last spectrum reported in both parts has been collected 120 s after the polymerization start, with IR spectroscopy we are monitoring only the time interval corresponding to region 2a in Fig. 3.

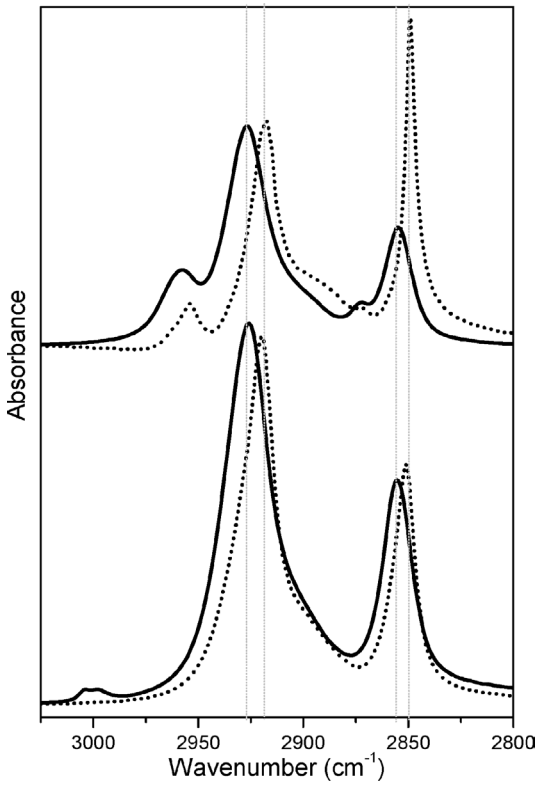

Fig. 5. FTIR spectra, in the $\nu(CH_2)$ region, of the polymeric chains growing on catalyst **S** and on catalyst **T** (bottom part, full and dotted lines, respectively). For comparison, also the spectra of *n*-hexadecane and of tritriacontane (characterized by a ratio $CH_3/CH_2 = 2/14$ and 2/31, respectively) are reported (top part, full and dotted lines, respectively). The gray vertical lines, centered on the main spectroscopic features of the two reference samples, show the frequency shifts which characterize the chains growing on catalyst **S** and **T**.

Table 1
Peak positions (cm^{-1}) for the antisymmetric and symmetric CH_2 stretching modes in different reference samples and in the polymeric chains growing on catalysts **S** and **T**

CH stretching mode	PE		Hexadecane[b]	Tritriacontane[b]	PE chains on catalyst **S**[b]	PE chains on catalyst **T**[b]
	Crystalline[a]	Liquid[a]				
$\tilde{\nu}_a(CH_2)$	2920	2928	2927	2918	2927	2919
$\tilde{\nu}_s(CH_2)$	2850	2856	2855	2849	2856	2850

[a] From Ref. [67].
[b] This work.

increased conformational disorder. For example, the peak position for the $\nu_a(CH_2)$ mode of a crystalline PE (characterized by a high conformational order) is 8 cm^{-1} lower than that for the liquid state (characterized by a lower conformational order), as reported in Table 1. The same holds for the $\nu_s(CH_2)$ mode. Similar results have been found in IR studies of the effect of molecular conformation of pure hydrocarbons [63–66] and in IR spectra collected on self-assemblied monolayers (SAMs) [67–69].

Porter et al. [67] reported an IR study on *n*-alkanethiolate SAMs on gold clusters for various *n*-alkyl chain lengths ($n = 3$ to 21). By comparing the $\tilde{\nu}(CH_2)$ peak positions, the authors demonstrated that there is a definite trend toward higher peak frequencies with decreasing length of the alkyl chain. The difference between the peak positions for the $n = 5$ and $n = 21$ alkyl thiols is almost 4 cm^{-1}. The authors concluded that shorter *n*-alkyl chains ($n = 3, 5$) are highly disordered and resemble free *n*-alkanes, whereas longer chains are more conformationally ordered. For $15 < n < 21$, the average local environment of an individual chain was very similar to that existing in the bulk crystalline phase. Similar results were obtained by Singh et al. [68,69], who examined silica gels chemically modified with *n*-alkyl chains of various lengths ($n = 8$ to 30). The difference between the position of the absorption maxima for the C8 and C30 modified silica gels was 6 cm^{-1}, again implying large differences in the degree of conformational order in the attached alkyl moieties. The conformational disorder was relatively high near the silica surface, decreased in the center of the chain, and increased once again near the chain end, a fact that can be attributed mainly to better chain packing in the inner section of the longer alkyl chains. The common idea resulting from these previous works is that longer alkyl chains obviously have greater conformational order. This trend can be derived directly from the CH_2 stretching data monitoring the shift of the absorption band maxima toward higher frequencies on alkyl chain length reduction.

From Fig. 5 and Table 1, it is clear that the position of the $\nu_a(CH_2)$ band is 8 cm^{-1} higher for chains formed on catalyst **S** with respect to those growing on catalyst **T**. A shift of 6 cm^{-1} is observed for the $\nu_s(CH_2)$ band. The comparison of all the data reported in Table 1 and the results discussed earlier suggest that the first polymeric chains growing on sample **T** are characterized by a high conformational order, so the average local environment of an individual PE chain is very similar to that existing in the bulk crystalline PE. This suggests that on sample **T**, long polyethylene chains formed on the fastest Cr^{II}_B sites interact in a manner similar to the interaction occurring in the solid polyethylene. This explains both the narrowness and the low frequency values of the $\nu(CH_2)$ bands. Conversely, on sample **S**, the slower C_2H_4 insertion ability of a greater number of Cr sites (Cr^{II}_A) is responsible for the presence of a great number of shorter chains characterized by higher conformational disorder, so that the average local environment appears similar to that of liquid PE. This explains the broader character of the $\nu(CH_2)$ bands and the higher $\nu(CH_2)$ values of the polymeric chains in the first stages of polymerization.

We have attempted to represent these concepts in Fig. 6, which reports a model of the Cr/SiO_2 surface carrying some polymeric chains. The average distance between Cr sites on the silica surface was set at about 10 Å, as would be expected for a loading of 1 wt% on a standard silica with a surface area of about 400 $m^2\,g^{-1}$. Not all of the Cr sites are carrying a polymeric chain, because only a fraction of the sites are active in C_2H_4 polymerization. For catalyst **S** (see Fig. 6a), the majority of the Cr sites are represented as carrying short, disordered chains. For catalyst **T** (see Fig. 6b), most of the Cr sites carry long chains, which interact with one another as in solid polyethylene. This property is evident when comparing the chains contained in the gray boxes in Fig. 6b with Fig. 6c, which reports two chains of crystalline polyethylene [70]. Note, however, that the picture has only qualitative value; that is, no attention has been given to the oxidation state of the Cr sites carrying the polymeric chains or to the nature of the first oligomeric products. In addition, the fraction of active Cr sites has been greatly increased for graphical reasons.

4. Conclusions

The present work shows that it is possible to determine a relationship between the structure of the Cr(II) precursors of the active sites, the catalytic performance of Phillips type catalysts, and the properties of the obtained polymers. In particular, we note the following conclusions:

1. The Cr^{II}_B sites show a higher tendency to insert a third ligand into their coordination sphere with respect to the Cr^{II}_A sites. This has been demonstrated in the case of CO, but we can reasonably imagine that it also could occur in the case of C_2H_4, the two molecules having a comparable strength of interaction with Cr(II).
2. The catalyst activation procedure has an important effect on varying the relative distribution of the Cr sites on the silica surface and their local environment. In particular, on thermal treatment after reduction, a complex $Cr^{II}_A \rightarrow Cr^{II}_B \rightarrow$

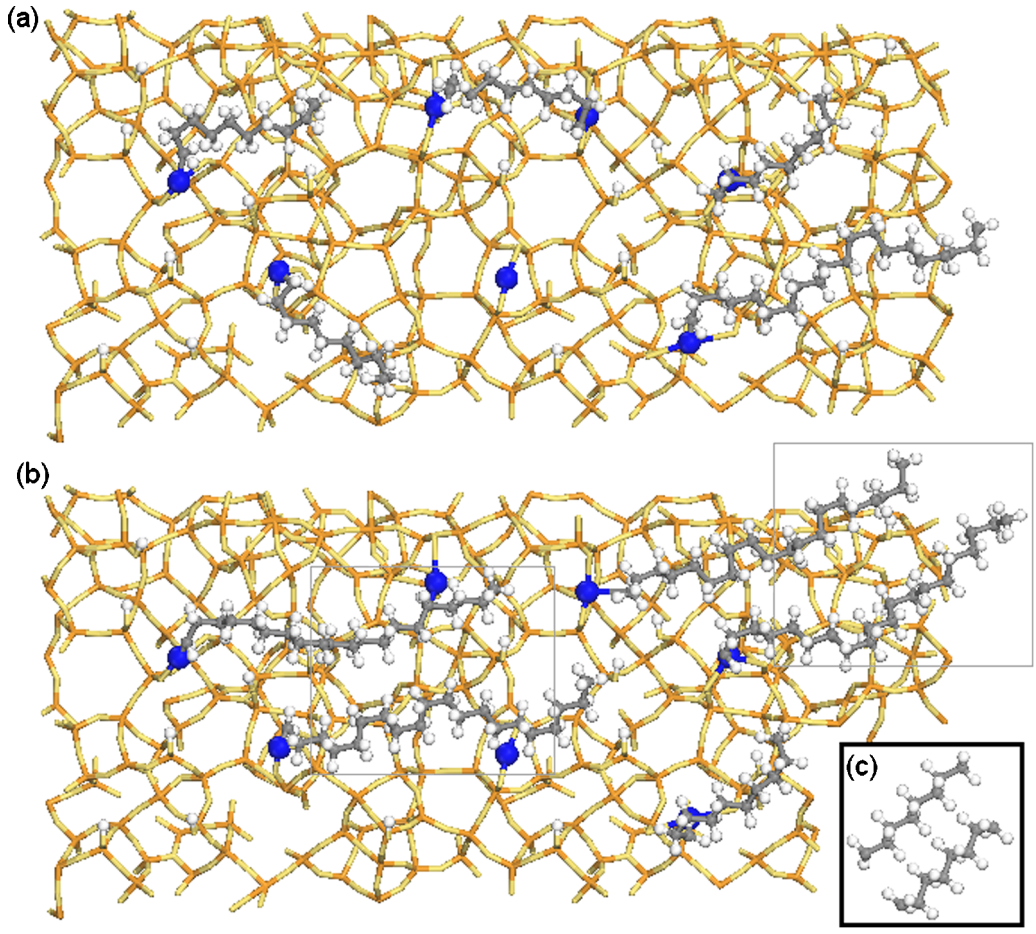

Fig. 6. Qualitative representation of the surface of catalysts **S** and **T** (parts a and b, respectively) carrying some polymeric chains. Red and yellow sticks connect together silicon and oxygen atoms respectively; the big blue balls represent Cr(II) ions, while the little gray and white balls represent carbon and hydrogen atoms, respectively. Gray rectangles in part (b) highlight the regions in which the polymeric chains are interacting at a distance (average C–C distance of 4.0 Å) in the same order of that characterizing crystal polyethylene (part c) [70].

Cr^{II}_C transformation is obtained. Overall, a great fraction of the Cr^{II}_A sites is converted into more shielded Cr^{II}_C sites, inactive in ethylene polymerization, and less abundantly into Cr^{II}_B sites.

3. In the first stages of the polymerization reaction, catalyst **T** inserts the C_2H_4 molecules faster than catalyst **S**. From points 1 and 2, we can infer that the higher activity presented by catalyst **T** in the first stages of the polymerization is due to the presence of an increased number of Cr^{II}_B sites. The B family sites present on the **T** sample have slightly different structures than those present on **S** sample. Therefore, the rate in the ethylene insertion seems strongly related to the ability of the Cr sites to insert a third ligand into their coordination sphere (i.e., to displace a weaker ligand).
4. The higher polymerization rate demonstrated by catalyst **T** in the first stages of the reaction accounts for the growth of longer and more ordered polymeric chains with respect to the standard case, as demonstrated by the FTIR spectra of the growing polymers.
5. The Cr^{II}_A sites are active in ethylene polymerization; however, they are characterized by slower insertion rates. This explains why after about 120 s, catalyst **S** becomes more active than catalyst **T**.

Points 1–5 confirm some of the phenomenological observations stated previously, such as the ability of the Phillips catalyst to produce PE characterized by a broad molecular weight (MW) distribution and the disactivating effect, in the industrial time scale, of thermal treatment after reduction. The novelty of this work is that it links different observations from different techniques to explain the origin of well-known phenomena. In particular:

(a) It has been shown that on the Phillips catalyst, a distribution of Cr(II) sites, all active in ethylene polymerization but characterized by different polymerization rates, is present. These sites are responsible for the production of polymer chains of differing chain lengths and thus differing MWs, and this is basically the origin of the broad MW distribution that characterizes the PE obtained with the Phillips catalyst. Toward this end, it is useful to recall that several current research activities involve the design of new ligands to reduce the complexity of the Cr/SiO_2 surface [71–74]. In general, Cr(III) complexes are involved, which, in combination with methylalumoxane (MAO), give extremely active catalysts. This approach leads to a reduction in the active site distribution and in some cases to the appearance of a single-site

catalytic behavior [74], which is uncommon for a heterogeneous system. The drastic reduction in the diversity of the active Cr sites generally existing on the silica surface is responsible of the production of a polymer characterized by a narrow MW distribution, thus confirming our previous statements.

(b) Furthermore, it has been confirmed that the lower activity of catalyst **T** on an industrial time scale is due to the absence of Cr^{II}_{A} sites, as has been suggested previously. However, the Cr^{II}_{A} sites do not provide the fastest ethylene polymerization, contrary to what has been believed up to now, and this fact has been related to the scarce tendency to insert a third ligand into the coordination sphere. To change the population of Cr(II) sites, an alternative strategy to the variation of the activation procedure, discussed herein, may be to insert suitable dopant ions inside the silica support, a method that has already been adopted in industry. In this regard, the results reported herein demonstrate that IR spectroscopy of probe molecules can be a useful tool for characterizing the distribution and structure of the Cr sites and thus for predicting the catalytic activity of the system.

Finally, the results illustrated in this work provide some new perspective regarding the solution of the problem of the initiation mechanism on the Phillips catalyst. The Cr^{II}_{A} sites, being slower in ethylene insertion compared with Cr^{II}_{B} sites, are also the most suitable for the spectroscopic investigation of the precursor species present in the very initial stages of the polymerization reaction. Therefore, all efforts in identifying the initiation mechanism should pass through the maximization of the fraction of Cr^{II}_{A} sites.

Acknowledgments

The authors thank M. Salvalaggio (Polimeri Europa, Novara, I) for fruitful discussions and Novara Technology for the silica aerogel material.

References

[1] E. Groppo, C. Lamberti, S. Bordiga, G. Spoto, A. Zecchina, Chem. Rev. 105 (2005) 115.
[2] K.H. Theopold, Chemtech 27 (1997) 26.
[3] B.M. Weckhuysen, R.A. Schoonheydt, Catal. Today 51 (1999) 215.
[4] M.P. McDaniel, Adv. Catal. 33 (1985) 47.
[5] V.J. Ruddick, P.W. Dyer, G. Bell, V.C. Gibson, J.P.S. Badyal, J. Phys. Chem. 100 (1996) 11062.
[6] V.J. Ruddick, J.P.S. Badyal, J. Phys. Chem. B 101 (1997) 9240.
[7] A.B. Gaspar, R.L. Martins, M. Schmal, L.C. Dieguez, J. Mol. Catal. A 169 (2001) 105.
[8] A.B. Gaspar, L.C. Dieguez, Appl. Catal. A 227 (2002) 241.
[9] A.B. Gaspar, J.L.F. Brito, L.C. Dieguez, J. Mol. Catal. A 203 (2003) 251.
[10] B.P. Liu, Y.W. Fang, M. Terano, J. Mol. Catal. A 219 (2004) 165.
[11] A. Zecchina, E. Garrone, G. Ghiotti, C. Morterra, E. Borello, J. Phys. Chem. 79 (1975) 966.
[12] A. Zecchina, E. Garrone, C. Morterra, S. Coluccia, J. Phys. Chem. 79 (1975) 978.
[13] A. Zecchina, E. Garrone, G. Ghiotti, S. Coluccia, J. Phys. Chem. 79 (1975) 972.
[14] J.P. Hogan, J. Polym. Sci. 8 (1970) 2637.
[15] R. Merryfield, M.P. McDaniel, G. Parks, J. Catal. 77 (1982) 348.
[16] E. Groppo, C. Lamberti, S. Bordiga, G. Spoto, A. Zecchina, J. Phys. Chem. B 109 (2005) 15024.
[17] G. Ghiotti, E. Garrone, A. Zecchina, J. Mol. Catal. 46 (1988) 61.
[18] V.J. Ruddick, J.P.S. Badyal, J. Phys. Chem. B 102 (1998) 2991.
[19] S.L. Scott, J. Amor Nait Ajjou, Chem. Eng. Sci. 56 (2001) 4155.
[20] P. Cossee, J. Catal. 3 (1964) 80.
[21] H.L. Krauss, K. Hagen, E. Hums, J. Mol. Catal. 28 (1985) 233.
[22] R. Blom, A. Follestad, O. Noel, J. Mol. Catal. 91 (1994) 237.
[23] M. Kantcheva, V. Bushev, D. Klissurski, J. Catal. 145 (1994) 96.
[24] B.M. Weckhuysen, R.A. Schoonheydt, J.M. Jehng, I.E. Wachs, S.J. Cho, R. Ryoo, S. Kijlstra, E. Poels, J. Chem. Soc. Faraday Trans. 91 (1995) 3245.
[25] B.M. Weckhuysen, I.E. Wachs, R.A. Shoonheydt, Chem. Rev. 96 (1996) 3327.
[26] B. Rebenstorf, R. Larsson, Z. Anorg. Allg. Chem. 478 (1981) 119.
[27] G. Ghiotti, E. Garrone, G. Della Gatta, B. Fubini, E. Giamello, J. Catal. 80 (1983) 249.
[28] E. Garrone, G. Ghiotti, C. Morterra, A. Zecchina, Z. Naturforsh. B 42 (1987) 728.
[29] B. Rebenstorf, J. Mol. Catal. 66 (1991) 59.
[30] G. Ghiotti, E. Garrone, A. Zecchina, J. Mol. Catal. 65 (1991) 73.
[31] E. Garrone, S. Abello, E. Borello, G. Ghiotti, A. Zecchina, Mater. Chem. Phys. 29 (1991) 369.
[32] G. Spoto, S. Bordiga, E. Garrone, G. Ghiotti, A. Zecchina, G. Petrini, G. Leofanti, J. Mol. Catal. 74 (1992) 175.
[33] P. Zielinski, I.G.D. Lana, J. Catal. 137 (1992) 368.
[34] P.A. Zielinski, J.A. Szymura, I.G.D. Lana, Catal. Lett. 13 (1992) 331.
[35] C.S. Kim, S.I. Woo, J. Mol. Catal. 73 (1992) 249.
[36] A. Zecchina, G. Spoto, G. Ghiotti, E. Garrone, J. Mol. Catal. 86 (1994) 423.
[37] A. Zecchina, D. Scarano, S. Bordiga, G. Spoto, C. Lamberti, Adv. Catal. 46 (2001) 265.
[38] S. Bordiga, S. Bertarione, A. Damin, C. Prestipino, G. Spoto, C. Lamberti, A. Zecchina, J. Mol. Catal. A 204 (2003) 527.
[39] M.A. Vuurman, I.E. Wachs, D.J. Stufkens, A. Oskam, J. Mol. Catal. 80 (1993) 209.
[40] T.J. Dines, S. Inglis, Phys. Chem. Chem. Phys. 5 (2003) 1320.
[41] E. Groppo, A. Damin, F. Bonino, A. Zecchina, S. Bordiga, C. Lamberti, Chem. Mater. 17 (2005) 2019.
[42] A. Damin, F. Bonino, S. Bordiga, E. Groppo, C. Lamberti, A. Zecchina, ChemPhysChem 6 (2005), in press.
[43] E. Groppo, C. Prestipino, F. Cesano, F. Bonino, S. Bordiga, C. Lamberti, P.C. Thüne, J.W. Niemantsverdriet, A. Zecchina, J. Catal. 230 (2005) 98.
[44] E.M.E. van Kimmenade, A.E.T. Kuiper, Y. Tamminga, P.C. Thune, J.W. Niemantsverdriet, J. Catal. 223 (2004) 134.
[45] A.B. Gaspar, R.L. Martins, M. Schmal, L.C. Dieguez, J. Mol. Catal. A 169 (2001) 105.
[46] B. Fubini, G. Ghiotti, L. Stradella, E. Garrone, C. Morterra, J. Catal. 66 (1980) 200.
[47] http://www.novaratechnology.com/home.html.
[48] V. Bolis, A. Barbaglia, S. Bordiga, C. Lamberti, A. Zecchina, J. Phys. Chem. B 108 (2004) 9970.
[49] B. Rebenstorf, Acta Chem. Scand. A 31 (1977) 877.
[50] B. Rebenstorf, Acta Chem. Scand. A 43 (1989) 413.
[51] C.C. Chang, R.J. Kokes, J. Phys. Chem. 77 (1973) 49.
[52] T.A. Egerton, N. Sheppard, J. Chem. Soc. Faraday Trans. 70 (1974) 1357.
[53] Y. Kuroda, S. Konno, K. Morimoto, Y. Yoshikawa, J. Chem. Soc., Chem. Commun. (1993) 18.
[54] H. Miessner, J. Am. Chem. Soc. 116 (1994) 11522.
[55] G. Spoto, S. Bordiga, G. Ricchiardi, D. Scarano, A. Zecchina, F. Geobaldo, J. Chem. Soc. Faraday Trans. 91 (1995) 3285.
[56] F. Geobaldo, C. Lamberti, G. Ricchiardi, S. Bordiga, A. Zecchina, G. Turnes Palomino, C. Otero Arean, J. Phys. Chem. 99 (1995) 11167.
[57] C. Lamberti, S. Bordiga, M. Salvalaggio, G. Spoto, A. Zecchina, F. Geobaldo, G. Vlaic, M. Bellatreccia, J. Phys. Chem. 101 (1997) 344.
[58] Y. Kuroda, H. Maeda, Y. Yoshikawa, R. Kumashiro, M. Nagao, J. Phys. Chem. B 101 (1997) 1312.

[59] A. Zecchina, C. Otero Arean, G. Turnes Palomino, F. Geobaldo, C. Lamberti, G. Spoto, S. Bordiga, Phys. Chem. Chem. Phys. 1 (1999) 1649.
[60] H. Miessner, K. Richter, J. Mol. Catal. A 146 (1999) 107.
[61] B. Rebenstorf, Z. Anorg. Allg. Chem. 513 (1984) 103.
[62] J.A. Szymura, I.G. DallaLana, R. Fiedorow, P.A. Zielinski, Macromolecules 29 (1996) 3103.
[63] R.G. Snyder, J. Chem. Phys. 42 (1965) 1744.
[64] R.G. Snyder, J. Chem. Phys. 47 (1967) 1316.
[65] R.G. Snyder, S.L. Hsu, S. Krimm, Spectrochim. Acta 34A (1978) 395.
[66] R.G. Snyder, S.H. Strauss, C.A. Elliger, J. Phys. Chem. 86 (1982) 5145.
[67] M.D. Porter, T.B. Bright, D.L. Allara, C.E.D. Chidsey, J. Am. Chem. Soc. 109 (1987) 3559.
[68] S. Singh, J. Wegmann, K. Albert, K. Muller, J. Phys. Chem. B 106 (2002) 878.
[69] S. Neumann-Singh, J. Villanueva-Garibay, K. Muller, J. Phys. Chem. B 108 (2004) 1906.
[70] C.W. Bunn, Trans. Faraday Soc. 35 (1939) 482.
[71] D.S. McGuinness, V.C. Gibson, D.F. Wass, J.W. Steed, J. Am. Chem. Soc. 125 (2003) 12716.
[72] V.C. Gibson, C. Newton, C. Redshaw, G.A. Solan, A.J.P. White, D.J. Williams, Dalton Trans. (2003) 4612.
[73] D.J. Jones, V.C. Gibson, S.M. Green, P.J. Maddox, A.J.P. White, D.J. Williams, J. Am. Chem. Soc. 127 (2005) 11037.
[74] C.N. Nenu, B.M. Weckhuysen, Chem. Commun. (2005) 1865.